THE JOURNAL OF BIOLOGICAL CHEMISTRY VOL. 283, NO. 27, pp. 18711–18720, July 4, 2008
Printed in the U.S.A.

Protease-activated Receptor-2 Increases Exocytosis via Multiple Signal Transduction Pathways in Pancreatic Duct Epithelial Cells*

Received for publication, February 29, 2008, and in revised form, April 30, 2008 Published, JBC Papers in Press, April 30, 2008, DOI 10.1074/jbc.M801655200

Mean-Hwan Kim[‡1], Bo-Hwa Choi[§], Seung-Ryoung Jung[‡], Thomas J. Sernka[¶], Seunghwan Kim[‡], Kyong-Tai Kim[§], Bertil Hille[‖], Toan D. Nguyen[¶], and Duk-Su Koh[‡‖2]**

*From the [‡]Departments of Physics and [§]Life Science, POSTECH, Pohang 790-784, Republic of Korea and [¶]Veterans Affairs Puget Sound Health Care System and Departments of [‖]Physiology and Biophysics and **Medicine, University of Washington, Seattle, Washington 98195*

Protease-activated receptor-2 (PAR-2) is activated when trypsin cleaves its NH_2 terminus to expose a tethered ligand. We previously demonstrated that PAR-2 activates ion channels in pancreatic duct epithelial cells (PDEC). Using real-time optical fluorescent probes, cyan fluorescence protein-Epac1-yellow fluorescence protein for cAMP, $PH_{PLC\text{-}\delta1}$-enhanced green fluorescent protein for phosphatidylinositol 4,5-bisphosphate, and protein kinase Cγ (PKCγ)-C1-yellow fluorescence protein for diacylglycerol, we now define the signaling pathways mediating PAR-2 effect in dog PDEC. Although PAR-2 activation does not stimulate a cAMP increase, it induces phospholipase C to hydrolyze phosphatidylinositol 4,5-bisphosphate into inositol 1,4,5-trisphosphate and diacylglycerol. Intracellular Ca^{2+} mobilization from inositol 1,4,5-trisphosphate-sensitive Ca^{2+} stores and a subsequent Ca^{2+} influx through store-operated Ca^{2+} channels cause a biphasic increase in intracellular Ca^{2+} concentration ($[Ca^{2+}]_i$), measured with Indo-1 dye. Single-cell amperometry demonstrated that this increase in $[Ca^{2+}]_i$ in turn causes a biphasic increase in exocytosis. A protein kinase assay revealed that trypsin also activates PKC isozymes to stimulate additional exocytosis. Paralleling the increased exocytosis, mucin secretion from PDEC was also induced by trypsin or the PAR-2 activating peptide. Consistent with the serosal localization of PAR-2, 1 μM luminal trypsin did not induce exocytosis in polarized PDEC monolayers; on the other hand, 10 μM trypsin at 37 °C damaged the epithelial barrier sufficiently so that it could reach and activate the serosal PAR-2 to stimulate exocytosis. Thus, in PDEC, PAR-2 activation increases $[Ca^{2+}]_i$ and activates PKC to stimulate exocytosis and mucin secretion. These functions may mediate the reported protective role of PAR-2 in different models of pancreatitis.

Of the four protease-activated receptors (PARs),[3] G-protein-coupled receptors activated by proteolysis (1, 2), PAR-1 and PAR-3 are activated by thrombin, PAR-2 by trypsin and tryptase, and PAR-4 by both thrombin and trypsin. Trypsin and tryptase cleave within the extracellular NH_2 terminus of PAR-2 (in humans, at the arrow N-SKGR ↓ SLIGRL-C) to yield a tethered ligand (N-SLIGRL-C) that activates the cleaved receptor. In various tissues PAR-2 couples with PLC to hydrolyze PIP_2 into IP_3 and DAG. IP_3 in turn increases $[Ca^{2+}]_i$, whereas DAG activates PKC (2–4).

PAR-2 is highly expressed in several tissues including pancreas, kidney, intestine, liver, and heart (3) where it mediates both physiologic and pathologic functions (2, 5, 6). PAR-2 function in the pancreas is of particular interest because its activator, trypsin, is a digestive enzyme produced by pancreatic acina. In pancreatic ducts, which channel digestive enzymes from the acina into the duodenum and further secrete fluid and electrolytes into the lumen, we demonstrated that PAR-2 mediates the activation of Ca^{2+}-actived K^+ and Cl^- channels (7). In addition, we also demonstrated that exocytosis from PDEC is induced by $[Ca^{2+}]_i$ increases and by activation of protein kinases A and C (8, 9).

We now report that PAR-2 activation stimulates PLC-mediated hydrolysis of PIP_2 into IP_3 and DAG, increasing $[Ca^{2+}]_i$ via Ca^{2+} mobilization from intracellular stores and Ca^{2+} influx through store-operated Ca^{2+} channels (SOC) and activating PKC. Each of these signals promotes exocytosis and mucin secretion.

EXPERIMENTAL PROCEDURES

Cell Culture—Canine PDEC, originally derived from the accessory pancreatic duct of a dog, were cultured on Vitrogen-coated Transwell inserts above a confluent feeder layer of human gall bladder myofibroblasts, as previously obtained and

* This work was supported, in whole or in part, by National Institutes of Health Grants GM083913 and DK55885. This work was also supported by the R&D Medical Research Office of the Department of Veterans Affairs (Merit Review) and by Korea Science and Engineering Foundation Grant R01-2002-000-00285). The costs of publication of this article were defrayed in part by the payment of page charges. This article must therefore be hereby marked "*advertisement*" in accordance with 18 U.S.C. Section 1734 solely to indicate this fact.

[1] Supported in part by Brain Korea 21 and the Korea Research Foundation Grant KRF-2006-612-C00011.

[2] To whom correspondence should be addressed: Dept. of Physiology and Biophysics, School of Medicine, University of Washington, Health Sciences Bldg., Seattle, WA 98195-7290. Tel: 206-543-6661; Fax: 206-685-0619; E-mail: koh@u.washington.edu.

[3] The abbreviations used are: PAR-2, protease-activated receptor 2; AP, activating peptide; BAPTA-AM, 1,2-bis-(*o*-aminophenoxy) ethane-*N*,*N*,*N*′,*N*′-tetraacetic acid acetoxymethyl ester; BIS, bisindolylmaleimide; $[Ca^{2+}]_i$, intracellular Ca^{2+} concentration; CFP, cyan fluorescence protein; DAG, diacylglycerol; IP_3, inositol 1,4,5-trisphosphate; PDEC, pancreatic duct epithelial cells; PIP_2, phosphatidylinositol 4,5-bisphosphate; PLC, phospholipase C; PMA, phorbol 12-myristate 13-acetate; RP, reversed peptide; SOC, store-operated Ca^{2+} channels; YFP, yellow fluorescence protein; GFP, green fluorescent protein; EGFP, enhanced GFP; FRET, fluorescence resonance energy transfer; PKC, protein kinase C; R_p-8-Br-cAMPS, Rp isomer 8-bromoadenosine 3′,5′-cyclic-monophosphorothioate.

described (10). These non-transformed cells are well differentiated, polarized, and have been used extensively in our laboratories for studies of PDEC secretion and receptor function. Single-cell amperometry and Ca^{2+} photometry were performed using isolated single cells plated on Vitrogen-coated glass coverslips, whereas measurements of PKC activity and mucin secretion used monolayers of polarized cells grown on Transwell inserts. Cells were used between passages 10 and 30.

Solutions and Chemicals—Normal Ringer's solution, used in most experiments, contained 137.5 mM NaCl, 2.5 mM KCl, 2 mM $CaCl_2$, 1 mM $MgCl_2$, 10 mM D-glucose, and 10 mM HEPES, pH 7.3. In Ca^{2+}-free Ringer's solution, $CaCl_2$ was omitted, and 100 μM EGTA was added to remove contaminating free Ca^{2+}. Dimethyl sulfoxide was used to prepare stock solutions of 20 mM 1,2-bis-(*o*-aminophenoxy) ethane-*N*,*N*,*N*′,*N*′-tetraacetic acid acetoxymethyl ester (BAPTA-AM), 500 μM bisindolylmaleimide (BIS) I and V, 5 mM thapsigargin, and 5 mM ionomycin. PAR-2-activating peptide (AP, N-SLIGRL-C), corresponding to the tethered ligand of mouse PAR-2 and the reversed peptide (RP, N-LRGILS-C) were from Genemed Synthesis (South San Francisco, CA). Indo-1 acetoxymethyl ester (AM), Fura-2 AM, BAPTA-AM, and pluronic F-127 were from Molecular Probes (Eugene, OR), and PMA and BIS I were from Calbiochem. The remaining chemicals and culture reagents were from Sigma, including trypsin (type XIII from bovine pancreas, product number T-8642). Solution exchange was achieved with a local perfusion system that allowed complete exchange within 0.5 s (11). All experiments were performed at room temperature (22–24 °C) unless otherwise stated.

Measurement of cAMP Levels—PDEC were transfected with 0.5 μg/ml cDNA of the Epac1-camps probe (CFP-Epac1-YFP, a gift of Dr. M. Lohse, Würzburg University) (12). One day after the transfection cells were inspected with a Nikon inverted microscope designed for fluorescence resonance energy transfer (FRET). Cells were illuminated every 1 s at 436 nm to activate CFP. When cAMP binds to the probe, it increases the distance between CFP and YFP and reduces the energy transfer from CFP to YFP, so that the FRET ratio (CFP/YFP) reflects cellular cAMP concentration. CFP and YFP fluorescence were corrected for background fluorescence.

Measurement of PIP_2 and DAG—Plasma membrane PIP_2 and DAG were monitored using $PH_{PLC\text{-}\delta1}$-EGFP (GFP-PH) and PKCγ-C1-YFP (YFP-C1), the fluorescent translocation probes, respectively. For these experiments, PDEC on glass coverslips were transfected with cDNA (0.5–0.8 μg/ml for GFP-PH or 2 μg/ml for YFP-C1, gifts from Dr. T. Meyer, Stanford University) using 5 μg/ml Lipofectamine 2000 (Invitrogen) for 6–8 h and further incubated for 12 h. Cells overexpressing the fluorescent probes were detected with a confocal Leica TCS NT microscope and a 63× water immersion objective. GFP fluorescence was excited at 488 nm and detected at 510 nm; YFP was excited at 488 nm and detected at 535 nm. Images acquired every 5 s were analyzed with Metamorph (Universal Imaging Co.) to define the time course of average fluorescence intensity (F) of a cytoplasmic region, normalized to the intensity at the start of the experiment (F_o).

Measurement of $[Ca^{2+}]_i$—For single cell experiments, PDEC were loaded with 2 μM membrane-permeant Ca^{2+}-sensitive dye Indo-1 AM for 30 min. Single cells were excited at 365 nm at 1- or 2-s intervals and emitted fluorescence at 405 and 500 nm, detected using two photon-counting photomultiplier tubes. A cell-free region was used for background fluorescence correction. $[Ca^{2+}]_i$ was calculated as $K^* \times (R - R_{min})/(R_{max} - R)$, where R is the ratio of fluorescence at 405 nm/fluorescence at 500 nm, K^* is the effective dissociation constant, and R_{min} and R_{max} are the ratios at minimal and maximal $[Ca^{2+}]_i$ (13). R_{min}, R_{max}, and K^*, determined with cells perfused with K^+-rich external solutions containing 20 μM ionomycin and 5 μM thapsigargin plus 20 mM EGTA or 15 mM Ca^{2+} or with 20 mM EGTA and 15 mM Ca^{2+} were 0.334, 3.733, and 2874 nM, respectively ($n = 10–14$ cells for each measurement).

For $[Ca^{2+}]_i$ determination in PDEC monolayers, a dual-excitation single-emission dye, Fura-2, was used because only one digital camera (Pixelfly QE, Cooke) was available to detect fluorescence in this setup. After loading with Fura-2 AM dye (4 μM, 30 min at 37 °C), the PDEC monolayer and supporting Transwell inserts were mounted on top of two thin glass spacers (~150 μm) which, together with a glass slide at the bottom, formed a small chamber. Fura-2 fluorescence was excited at 340 and 380 nm and detected at 510 nm. In this imaging system only changes in $[Ca^{2+}]_i$ could be determined through the ratio of fluorescence at 340 and 380 nm, as no cell-free region was present for background determination and correction.

Measurement of Exocytosis—Carbon-fiber amperometry, which detects the fusion of single secretory vesicles with the plasma membrane in real time, was used to measure exocytosis. Dopamine was artificially preloaded into secretory vesicles (8, 14) so that its exocytotic release from vesicles could be monitored electrochemically as spikes of oxidation current at the tip of a carbon-fiber electrode (15). Amperometry used mostly single cells in subconfluent cultures with visual control provided by an inverted microscope. If trypsin treatment lasted longer than 5 min, the few cells (<10%) that became partly detached were not analyzed. For PDEC monolayers, the supporting Transwell insert applied firm pressure from a metal grid, preventing the leak of test solutions into the serosal side. Solutions were exchanged within 0.5 s using a local perfusion system, and the temperature of the solution was controlled as necessary. Application of 10 μM trypsin to the carbon fiber electrode did not induce any oxidative current; in addition, oxidative currents induced by 10 μM dopamine did not change after exposure of the electrode to 10 μM trypsin for 20 min at 35 °C (40 pA before *versus* 38 pA after trypsin treatment, at a holding potential of 400 mV).

The amperometric spikes were detected and measured using the IGOR Pro (Wave Metrics). All events detected by amperometry were also visually confirmed. "Rate of exocytosis" is the number of amperometric spikes observed within a 30-s time bin; "normalized rate of exocytosis" is the rate of stimulated exocytosis divided by average rate of exocytosis in the control Ringer's solution in each experiment; "relative exocytosis" is the ratio of the average rate of exocytosis stimulated by agonists, such as trypsin and AP (for 3 or 6 min) over the rate under control conditions (for 3 min). Relative exocytosis values >1 or <1 indicate, respectively, increased exocytosis or decreased

exocytosis. In Fig. 5*D* and 9*D*, early (0–3 min in test solution) and late (3–6 min) responses were analyzed separately.

Measurement of Mucin Secretion—Mucins synthesized by confluent PDEC were labeled for 24 h with acetyl-D-[^{3}H]glucosamine (~2 μCi/Transwell insert; MP Biomedicals). The cell monolayers were then washed with 100 mM NaCl and 20 mM Na_2HPO_4, pH 7.4, reincubated in a serum-free medium, and treated for 1 h with different agents at 37 °C. After this incubation, medium in the luminal compartment was collected, and cell debris was removed by centrifugation at 1000 × *g* for 5 min. The labeled glycoproteins contained in a 0.5-ml aliquot of this sample were next precipitated with 10% trichloroacetic acid, 1% phosphotungstic acid, and the associated radioactivity was determined in a scintillation counter. This radioactivity, extrapolated to the total volume of the overlying medium, is expressed as a percentage of the control values obtained with unstimulated cells.

PKCα and PKCδ Kinase Assay—PDEC on Transwell inserts were washed with a serum-free medium, harvested with a rubber policeman, and collected through centrifugation at 1000 × *g* for 10 min. The cells were lysed on ice for 40 min using a solution containing 150 mM NaCl, 1 mM EDTA, 1 mM EGTA, 20 mM Tris-HCl, 2.5 mM sodium pyrophosphate, 1 mM β-glycerol phosphate, 1 mM phenylmethylsulfonyl fluoride, 1 mM NaF, 1 mM Na_3VO_4, 10 mM μg/ml aprotinin, 10 mM μg/ml pepstatin A, 10 mM μg/ml leupeptin, and 1% Triton X-100, pH 7.5, and the cell debris was removed by centrifugation at 22,250 × *g* for 15 min. PKC isoforms (α and δ) contained in 40 μg of protein in the resulting supernatant were immunoprecipitated for 16 h at 4 °C using antibodies against these PKC isoforms coupled to protein A-Sepharose beads (Santa Cruz Biotechnology). The immunoprecipitate was then washed 4 times in cold lysis buffer and subjected to PKC kinase assays consisting of 30 min of incubation at 30 °C in a 30-μl mixture of 5 mM β-glycerol phosphate, 2 mM dithiothreitol, 0.1 mM sodium orthovanadate, 10 mM $MgCl_2$, 25 mM Tris-HCl, pH 7.5, containing 50 μM ATP, 1 μCi of [γ-^{32}P]ATP, and 200 μg/ml histone H1. Phosphorylated histone H1 was resolved on 14% SDS-polyacrylamide gels, detected by autoradiography, and quantitated after normalization for total isoform of PKC.

Paracellular Permeability for Large Molecules across PDEC Monolayers—A Transwell insert supporting a PDEC monolayer was mounted on top of the thin (~170 μm) glass spacer forming the serosal compartment. Paracellular permeability was monitored as leakage of dextran-fluorescein from the luminal to serosal compartment, monitored in the lower part of the serosal compartment through an objective lens with high optical sectioning (100× oil immersion, NA 1.3). Fluorescein was excited at 480 nm (Polychrome, TILL Photonics).

Data Analysis—Numerical values are given as the means ± S.E.; *n* is the number of cells measured unless otherwise stated. Statistically significant differences ($p \leq 0.05$ (*)) between the means of two groups were determined by Student's two-tailed, unpaired *t* test.

RESULTS

Trypsin Does Not Increase cAMP in PDEC—Although PAR-2 effects are classically mediated through increased $[Ca^{2+}]_i$,

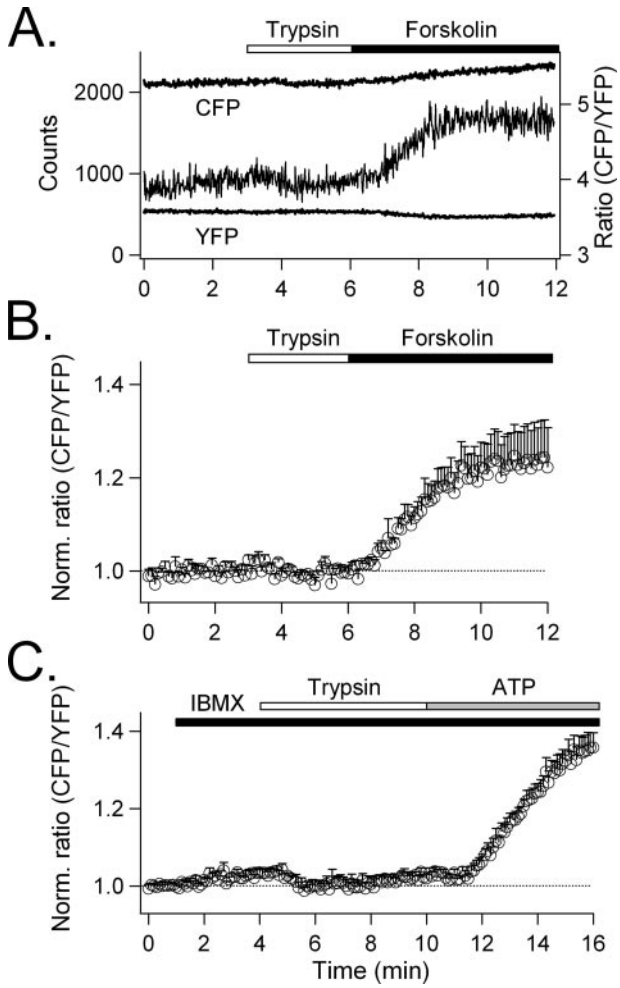

FIGURE 1. **Measurement of cAMP in single PDEC activated by trypsin.** PDEC were transiently transfected with Epac1-camp. The FRET ratio (CFP/YFP) indicates the cytoplasmic cAMP level. *A*, cells were stimulated with 1 μM trypsin and subsequently with 20 μM forskolin. A representative recording of CFP and YFP fluorescence and their ratio (CFP/YFP) is shown. *B*, average normalized FRET ratio ($n = 4$). *C*, cells were sequentially treated with 1 μM trypsin and 100 μM ATP in the presence of 100 μM isobutylmethylxanthine (*IBMX*; $n = 5$).

PAR-2 activation has been associated with increased cAMP and PKA activation in some cell types (16–18). Intracellular cAMP in dog PDEC stimulated by trypsin was, therefore, directly determined using FRET photometry (12). With this method, when a mosaic protein, which includes CFP, YFP, and intermediate Epac1, binds cAMP at the Epac1-camps domain, the distance between CFP and YFP will increase, reducing the energy transfer from CFP to YFP and increasing the ratio of fluorescence CFP/YFP. As shown in Fig. 1, *A* and *B*, this ratio did not increase after treatment with 1 μM trypsin but clearly increased after subsequent control treatment with 20 μM concentrations of the adenylyl cyclase activator, forskolin. In Fig. 1*C*, when 100 μM isobutylmethylxanthine was used to block cAMP degradation, 1 μM trypsin still did not increase cAMP. In contrast, cAMP clearly increased when, as a positive control, 100 μM ATP was used to activate the $P2Y_{11}$ receptor (19).

Trypsin Induces the Hydrolysis of PIP_2 to IP_3 and DAG—In different tissues PAR-2 appears to couple with $G_{q/11}$ to activate PLC-β and cleave the membrane phospholipids PIP_2 into IP_3 and DAG (2). Our prior observation that PAR-2 stimulates

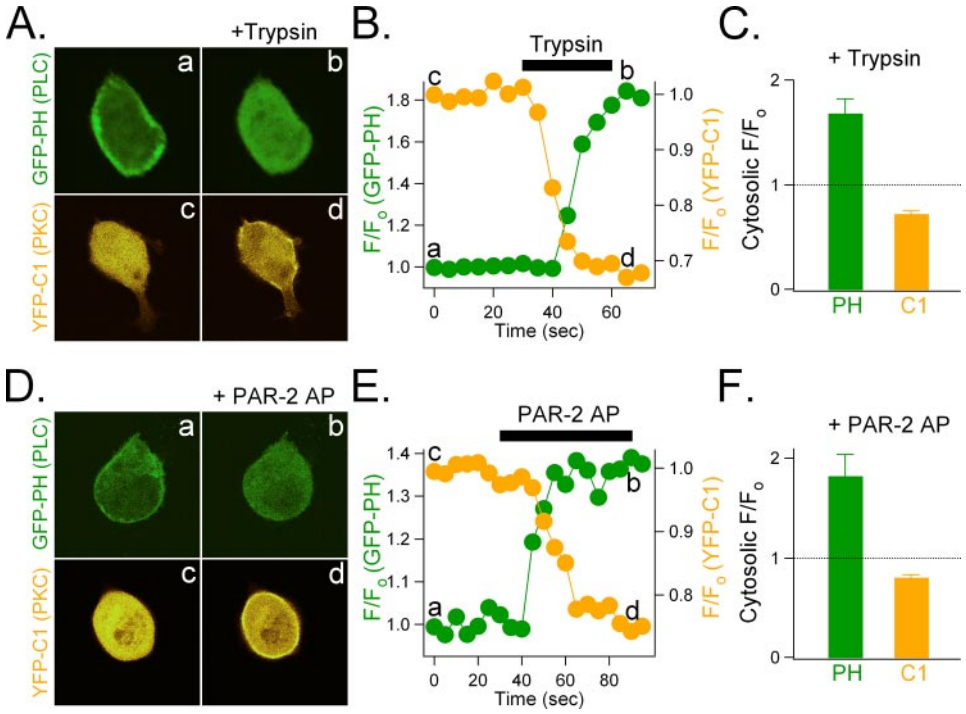

FIGURE 2. **Trypsin-induced depletion of plasma membrane PIP_2 and formation of plasma membrane DAG and cytoplasmic IP_3.** *A*, confocal fluorescence images of the GFP-PH probe for PIP_2/IP_3 before (*a*) and after (*b*) 1 μM trypsin treatment and of the YFP-C1 probe for DAG before (*c*) and after (*d*) trypsin treatment. *B*, time courses of cytoplasmic fluorescence, normalized to the initial fluorescence (F/F_o). *C*, average cytoplasmic fluorescence ratio (F/F_o), with *F* being the maximal fluorescence after trypsin treatment (only responsive cells were analyzed: 6/6 cells for GFP-PH and 9/12 cells for YFP-C1). *D*, fluorescence images of the GFP-PH probe before (*a*) and after (*b*) 100 μM PAR-2 AP stimulation and of the YFP-C1 probe before (*c*) and after (*d*) PAR-2 AP. *E*, time course of cytoplasmic ratio. *F*, average cytoplasmic fluorescence ratio after PAR-2 AP treatment; the majority of tested cells showed reciprocal translocation of GFP-PH (7/8 cells) and YFP-C1 (3/4).

Ca^{2+}-activated Cl^- and K^+ channels on PDEC suggests a role for PLC in these cells as well. Fluorescent optical probes for PIP_2/IP_3 ($PH_{PLC\text{-}\delta1}$-EGFP) and DAG (PKCγ-C1-YFP) were, therefore, expressed in PDEC to verify this possibility (Ref. 20, Fig. 2).

Confocal microscopy demonstrated that the $PH_{PLC\text{-}\delta1}$-EGFP probe, at rest, was localized to the plasma membrane, where it would be bound by PIP_2. Within 20 s of trypsin treatment, the probe migrated from the membrane to the intracellular space, indicating a rise of cytosolic IP_3 and a fall of membrane PIP_2 due to PIP_2 hydrolysis (Fig. 2, *A* and *B*, *green symbols*). In parallel, PKCγ-C1-YFP migrated from the intracellular space to the plasma membrane, indicating generation of membrane DAG by PIP_2 hydrolysis (Fig. 2, *A* and *B*, *yellow symbols*). Similar results were obtained in cells stimulated with PAR-2 AP (Fig. 2, *D* and *E*). Figs. 2, *C* and *F*, graphically summarize the migration of these fluorescent markers after PAR-2 activation by trypsin and PAR-2 AP, respectively.

Trypsin Increases $[Ca^{2+}]_i$—IP_3 generated after PLC-mediated hydrolysis of PIP_2 may increase $[Ca^{2+}]_i$ through two mechanisms, rapid Ca^{2+} mobilization from intracellular Ca^{2+} stores (*e.g.* endoplasmic reticulum) followed by slow Ca^{2+} influx through SOC (4). The biphasic increase in $[Ca^{2+}]_i$ observed previously when PDEC are stimulated by trypsin (a sharp peak slowly declining to a sustained increase) may reflect the contribution of both mechanisms (7). Indo-1 Ca^{2+} photometry was, therefore, used to determine the relative contributions of these two mechanisms to increased $[Ca^{2+}]_i$ in single cells.

Fig. 3*A* illustrates the typical biphasic $[Ca^{2+}]_i$ changes previously observed in single cells in response to 1 μM trypsin; that is, an initial rapid increase within 1–2 s from a base line of ~0.1 μM Ca^{2+} to a peak value of >1 μM (phase 1) followed by a slow decline toward a steady-state sustained increased (phase 2). Four of 10 cells tested also exhibited $[Ca^{2+}]_i$ oscillations in phase 2 (7).

In Fig. 3*B* Ca^{2+} in the external medium was removed to determine the contribution of Ca^{2+} influx. The initial peak $[Ca^{2+}]_i$ increase in phase 1 was preserved (1.2 ± 0.2 μM, $n = 8$ *versus* 1.7 ± 0.2 μM, $n = 10$ in 2 mM Ca^{2+}, shown in *panel A*, $p = 0.11$), but the late sustained $[Ca^{2+}]_i$ increase in phase 2 was abolished. When 2 mM Ca^{2+} was added back to the external medium, the phase 2 increase redeveloped, showing that it was due to Ca^{2+} entry through SOC.

In Fig. 3*C*, the role of SOC in mediating this Ca^{2+} influx was verified using 10 μM La^{3+}, which selectively blocks epithelial SOC (21). Similar to external Ca^{2+} depletion in Fig. 3*B*, La^{3+} abolished the late sustained $[Ca^{2+}]_i$ increase without affecting the initial peak (1.7 ± 0.2 μM, $n = 5$ *versus* 1.7 ± 0.2 μM without La^{3+}, $n = 10$, $p = 0.89$). The contribution of SOC to $[Ca^{2+}]_i$ increases is estimated as the difference in $[Ca^{2+}]_i$ response in the presence and absence of La^{3+}, as shown by the *dotted line*.

Thus, when trypsin activates PAR-2 on PDEC, the initial rapid, peaked $[Ca^{2+}]_i$ increase results from mobilization from intracellular stores. It is followed by Ca^{2+} influx mediated through the SOC.

Trypsin Stimulates Exocytosis through Increased Cytosolic Ca^{2+}—In PDEC we previously demonstrated that the increased $[Ca^{2+}]_i$ stimulated by PAR-2 activates Cl^- and K^+ channels (7) and that different signaling pathways, including cAMP, Ca^{2+}, and PKC, can promote exocytosis (8, 9, 22). Therefore, we used sensitive single-cell amperometry to examine whether trypsin will stimulate exocytosis and to define the underlying signaling mechanisms.

Fig. 4 illustrates how fusion of single vesicles with the plasma membrane is detected as amperometric spikes (Fig. 4*A*); the rate of exocytosis is defined as the number of spikes within a 30-s time bin (Fig. 4*B*). Trypsin, at 1 μM, stimulated a rapid increase in the exocytosis rate. That peaked at 1–2 min and slowly decreased afterward to a sustained plateau even with trypsin continuously present. After trypsin removal exocytosis remained elevated for several minutes.

In Fig. 5*A*, when the rate of exocytosis for each experiment was normalized to the base-line rate and the resulting rates

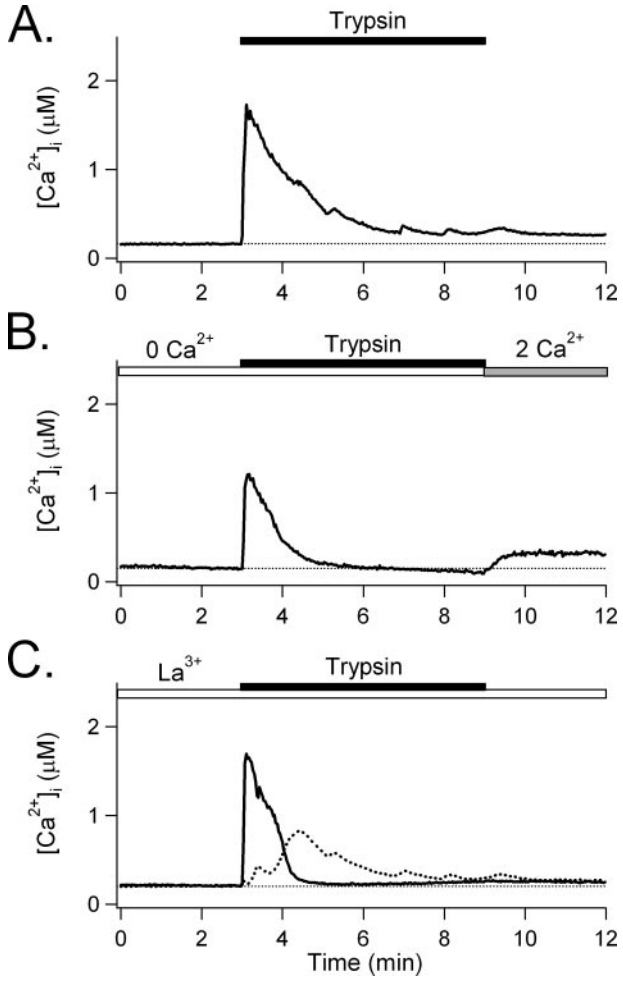

FIGURE 3. **Trypsin-induced $[Ca^{2+}]_i$ increases.** *A*, $[Ca^{2+}]_i$ increase evoked by trypsin. PDEC were treated with 1 μM trypsin (*bar*) in Ringer's solution containing 2 mM Ca^{2+}. $[Ca^{2+}]_i$, monitored using the Indo-1 ratiometric Ca^{2+} dye (averaged from 10 experiments). *B*, $[Ca^{2+}]_i$ increase by trypsin in the absence of extracellular Ca^{2+}. PDEC were treated with 1 μM trypsin in Ca^{2+}-free Ringer's solution (*open bar*). Extracellular Ca^{2+} was reinstated to 2 mM (*gray bar* at the end of the experiment (averaged from 8 experiments). *C*, $[Ca^{2+}]_i$ increase by trypsin in the presence of 10 μM La^{3+}. PDEC were preincubated with La^{3+} and treated with 1 μM trypsin in Ringer's solution containing 2 mM Ca^{2+} and La^{3+} ($n = 5$). The *solid trace* is $[Ca^{2+}]_i$ averaged from five experiments; the *dotted line* is the difference between the solid $[Ca^{2+}]_i$ *traces* in *A* and *C* and reflects La^{3+}-sensitive Ca^{2+} influx through SOC.

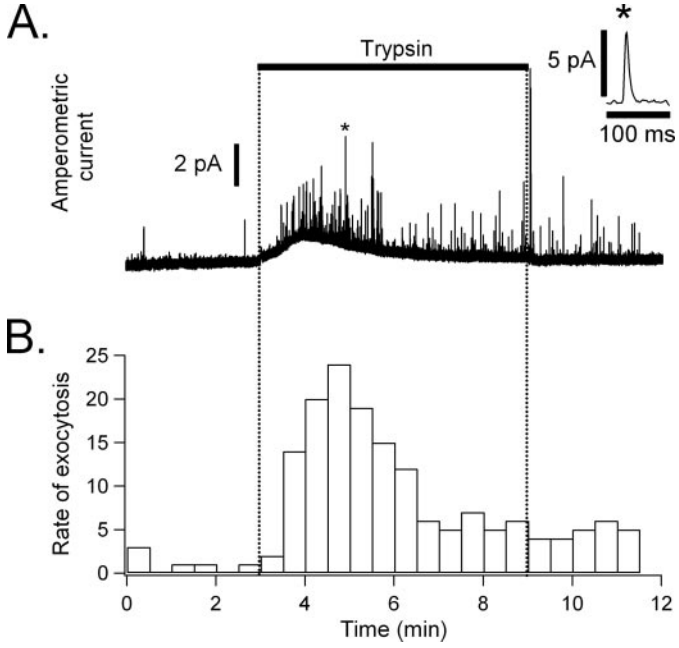

FIGURE 4. **Trypsin-induced exocytosis in individual PDEC.** *A*, amperometric spikes from a single PDEC treated with trypsin. Dopamine-loaded PDEC were treated with 1 μM trypsin (*bar*) in Ringer's solution containing 2 mM Ca^{2+}. Exocytotic events are exhibited as amperometric spikes; a small upward deflection of the base line during trypsin stimulation reflects contaminating dopamine released at remote sites diffusing to the electrode. *Inset*, one amperometric spike (*) is shown at an expanded time scale, illustrating fusion of a single vesicle. *B*, increase in the rate of exocytosis with trypsin treatment. The number of amperometric spikes per 30 s is compiled from the recording shown in *A*.

from different experiments were averaged, the relative exocytosis in the 6 min after the addition of trypsin increased from 1.0 to 5.6 ± 1.4 ($n = 14$). When Ca^{2+} influx through SOC was prevented by extracellular Ca^{2+} depletion or by La^{3+}, the exocytosis stimulated by trypsin was limited to the initial peaked increase (Fig. 5, *B* and *C*). Indeed, whereas trypsin treatment increased the relative exocytosis to 7.1 ± 1.7 for the first 3 min and 4.2 ± 1.2 for the next 3 min ($n = 14$, Fig. 5, *A* and *D*), without Ca^{2+} influx (Fig. 3, *B* and *C*), the corresponding relative exocytosis in the first 3 min still increased to 4.3 ± 1.4 in Ca^{2+}-free solution and 4.5 ± 0.9 in La^{3+}-containing solution. However, the increase of exocytosis in the following 3 min was abolished (0.6 ± 0.2 for Ca^{2+}-free, $n = 13$ and 0.9 ± 0.3 for La^{3+}, $n = 10$). These findings suggest that SOC-mediated Ca^{2+} influx maintains the late sustained increase in exocytosis evoked by trypsin.

Trypsin Also Stimulates Exocytosis through PKC—In addition to IP_3, PIP_2 hydrolysis generates DAG, which in turn activates PKC. We, therefore, investigated whether trypsin could induce exocytosis via PKC independent of a $[Ca^{2+}]_i$ increase. As shown in Fig. 6*A*, BAPTA-AM (20 μM), preloaded into PDEC to chelate intracellular Ca^{2+}, completely blocked the trypsin-induced increase in $[Ca^{2+}]_i$ (*solid line*) but did not abolish the increase in exocytosis in the first 3 min (relative exocytosis, 3.2 ± 0.9, $n = 21$, $p = 0.03$). Similarly, combined treatment with 5 μM thapsigargin (to deplete intracellular Ca^{2+} stores) plus 10 μM La^{3+} (to block SOC and Ca^{2+} influx) abolished the trypsin-induced $[Ca^{2+}]_i$ increase. Nevertheless, a residual increase of exocytosis in the first 3 min was still observed (1.7 ± 0.5, $n = 18$, $p = 0.01$, Fig. 6*B*). Thus, Ca^{2+} is not the sole signal that mediates trypsin-induced exocytosis.

To identify the mechanism underlying Ca^{2+}-independent stimulation of exocytosis, 100 nM BIS I, a PKC selective inhibitor, was used. It completely abolished the residual Ca^{2+}-independent exocytosis induced by trypsin in BAPTA-treated PDEC (0.9 ± 0.4; $n = 6$, Fig. 6, *C* and *D*). BIS V, an inactive BIS I analogue, did not reproduce this effect even at 500 nM (2.7 ± 0.7; $n = 9$, Fig. 6*D*). Another PKC blocker, calphostin C, also abolished Ca^{2+}-independent exocytosis (10 μM, 1.3 ± 0.3; $n = 7$). In addition, rottlerin, a selective inhibitor of the Ca^{2+}-insensitive PKCδ subtype (23), inhibited this Ca^{2+}-independent exocytosis as well (30 μM, 0.9 ± 0.3; $n = 6$). In contrast, 1 mM Rp-8-Br-cAMPS, a specific inhibitor of protein kinase A, failed to exhibit any significant effect (1 mM, 2.2 ± 0.4; $n = 13$, Fig. 6*D*).

Activation of PKC by trypsin was demonstrated by directly measuring the enzymatic activity of two isoforms of PKC in

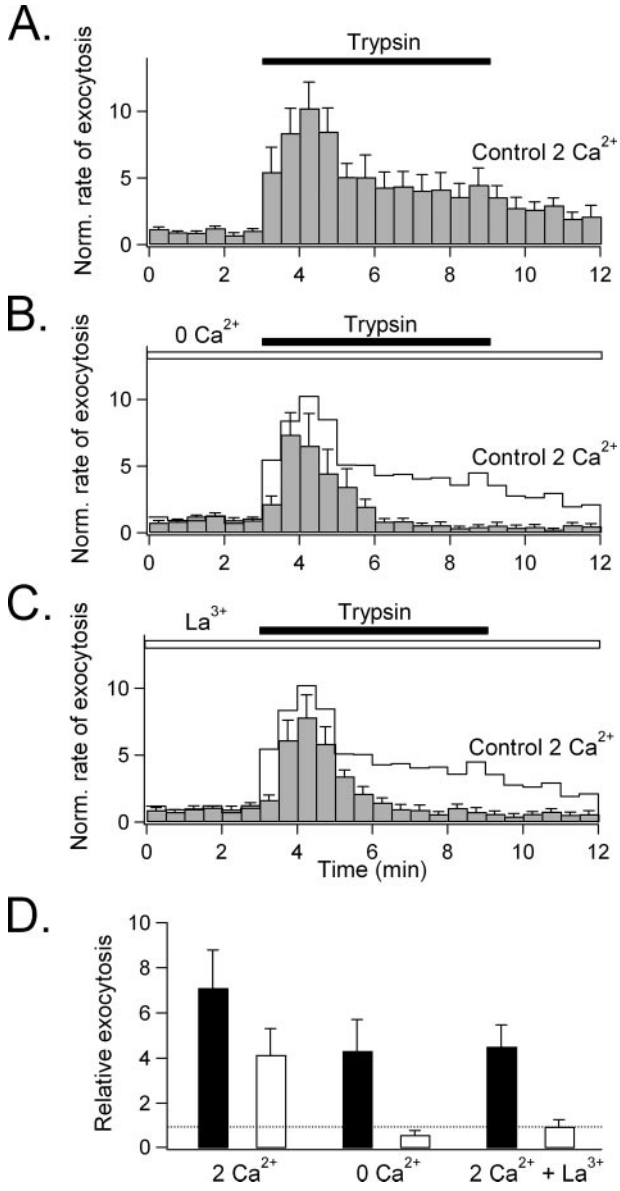

FIGURE 5. **Exocytosis induced by trypsin.** *A*, average normalized rate of exocytosis stimulated by trypsin ($n = 14$). Cells bathed in Ringer's solution containing 2 mM Ca^{2+} were stimulated with 1 μM trypsin. The exocytosis rate, normalized and then averaged from 14 experiments, showed a two-phase increase. *B*, exocytosis induced by trypsin in the absence of external Ca^{2+}. PDEC were treated with 1 μM trypsin in Ca^{2+}-free Ringer's solution and the resulting rates of exocytosis were normalized and then averaged from 13 experiments. For comparison, the normalized rate of exocytosis under the control condition, shown in *A*, is reproduced as a *solid line* and labeled *Control 2 Ca^{2+}*. *C*, exocytosis induced by trypsin in the presence of 10 μM La^{3+}. PDEC were preincubated with La^{3+} and treated with 1 μM trypsin in the presence of La^{3+}; the resulting rates of exocytosis were normalized and then averaged from 10 experiments. *D*, relative exocytosis evoked by trypsin under the conditions shown in *A–C*. Exocytosis stimulated by 1 μM trypsin was analyzed separately during the early (3–6 min, *filled bar*) and the late (6–9 min, open bar) phases. *2 Ca^{2+}* denotes relative exocytosis in Ringer's solution containing 2 mM Ca^{2+}, *0 Ca^{2+}* denotes exocytosis in Ca^{2+}-free Ringer's, and *2 Ca^{2+} + La^{3+}* denotes exocytosis in Ringer's containing 2 mM Ca^{2+} and 10 μM La^{3+}. The *broken line* indicates background exocytosis before trypsin treatment.

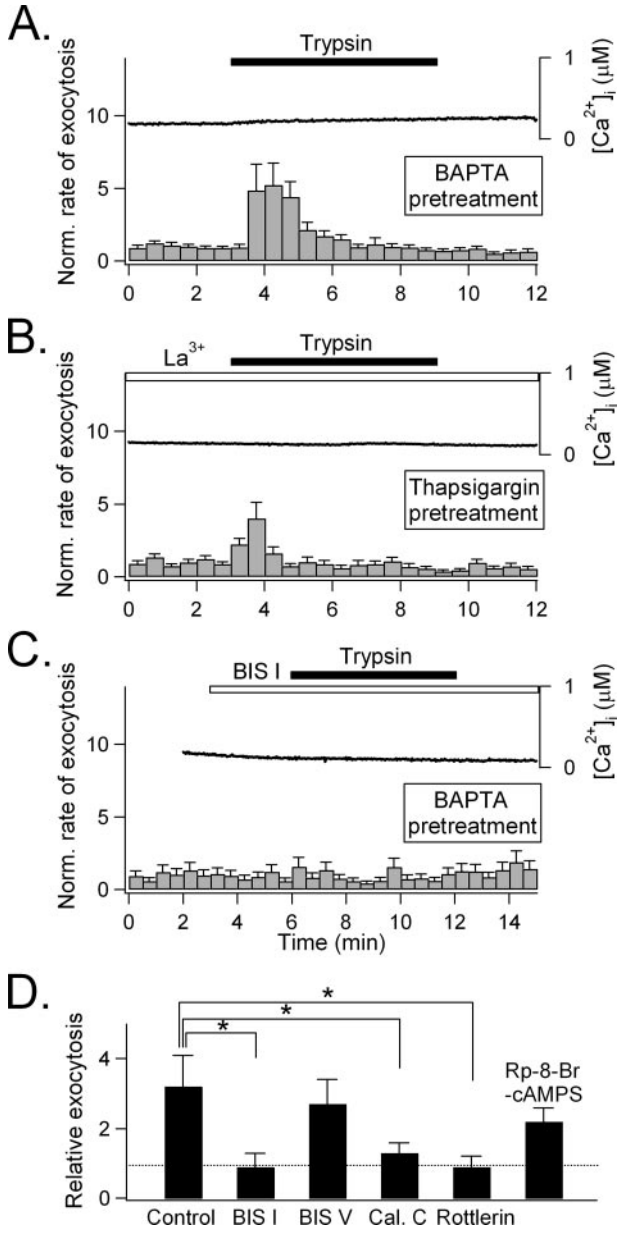

FIGURE 6. **Role of PKC in exocytosis induced by trypsin.** *A*, PDEC were preincubated with 20 μM BAPTA-AM for 1 h at 37 °C and then treated with 1 μM trypsin. $[Ca^{2+}]_i$ averaged from four cells (*solid line*). Exocytosis (*gray bars*) is the average from 21 cells. *B*, PDEC were pretreated with both 5 μM thapsigargin for 5 min to deplete intracellular Ca^{2+} stores and 10 μM La^{3+} to block Ca^{2+} influx through SOC and then treated with 1 μM trypsin. Similar to *panel A*, $[Ca^{2+}]_i$ was averaged from 3 cells, and exocytosis was averaged from 18 cells. *C*, PDEC were pretreated with 20 μM BAPTA-AM and then treated with 100 nM of the PKC inhibitor BIS I for 3 min before application of 1 μM trypsin. $[Ca^{2+}]_i$ was averaged from four cells, and exocytosis was averaged from 6 cells. *D*, mediation of Ca^{2+}-independent exocytosis by PKC, not PKA. PDEC pretreated with 20 μM BAPTA-AM and treated with 1 μM trypsin in the absence (control) or presence of different protein kinase inhibitors (100 nM BIS I, $n = 6$; 500 nM BIS V, an inactive BIS I analogue, $n = 9$; 10 μM calphostin C (*Cal. C*), $n = 6$; 30 μM Rottlerin, $n = 6$; 1 mM Rp-8-Br-cAMPS, $n = 13$). Relative exocytosis was calculated for the first 3 min after trypsin treatment. The *asterisk* (*) denotes the significant statistical difference compare with BAPTA control (*Control*, $p < 0.05$).

PDEC, α (a conventional PKC activated by Ca^{2+} and DAG) and δ (a novel isoform activated only by DAG). As displayed in Fig. 7*A*, the phosphorylation of histone H1 by PKCα (*panel A*) and by PKCδ (*panel B*) was significantly increased by 1 μM trypsin ($p = 0.04$ for PKCα and PKCδ). Thus, trypsin activation of conventional (*e.g.* PKCα) and novel (*e.g.* PKCδ) PKC isotypes may mediate the exocytosis stimulated by this protease via PAR-2.

PKC and Increased $[Ca^{2+}]_i$ Both Stimulate Exocytosis—We next examined the relative contributions and potential interac-

tion of the different trypsin-induced signals to exocytosis. To assess the role of Ca^{2+} influx, PDEC were preincubated in Ca^{2+}-free Ringer's solution containing 5 μM thapsigargin to deplete intracellular Ca^{2+} stores and fully activate SOC. After establishment of basal $[Ca^{2+}]_i$ in Ca^{2+}-free medium for 3 min, 2 mM Ca^{2+} was added to the medium, inducing a Ca^{2+} influx through the SOC. The $[Ca^{2+}]_i$ increased to >1 μM, exhibiting slow oscillatory fluctuations with a period of ~3 min (Fig. 8*A*, $n = 5$). This Ca^{2+} influx was mediated by SOC because it was observed only after significant depletion of Ca^{2+} stores by thapsigargin (the original criterion defining SOC) and was almost completely blocked by La^{3+} (10 μM, $n = 3$) or 2-aminoethoxydiphenyl borate (100 μM, $n = 6$) (data not shown).

Amperometric measurements in the thapsigargin-treated cells showed that the SOC-mediated $[Ca^{2+}]_i$ increase evoked only a modest amount of exocytosis (2.1 ± 0.4 for the initial 3 min of 2 mM Ca^{2+} repletion, Fig. 8, *A* and *C*). In contrast, when trypsin activated SOC, the $[Ca^{2+}]_i$ increase, even though smaller (<0.6 μM, Fig. 3, *A* and *C*), stimulated greater exocytosis (4.2 ± 1.2, $p < 0.01$, Fig. 5*D*). This difference suggests that the exocytosis evoked by trypsin might be potentiated by concurrent activation of PKC. Indeed, preincubation of PDEC with 10 nM phorbol myristate acetate (PMA), a PKC activator, potentiated the SOC-mediated exocytosis (4.2 ± 0.9, $n = 13$, Fig. 8, *B* and *C*). The PKC activation with this low concentration of PMA by itself had only a minor direct effect on exocytosis (1.3 ± 0.2, $n = 13$) and on SOC-mediated $[Ca^{2+}]_i$ increase (Fig. 8*B*). Thus, trypsin-induced Ca^{2+} influx through SOC produces a modest $[Ca^{2+}]_i$ increase that induced only a modest level of exocytosis. Its effect was magnified by PKC activation.

We next evaluated whether PKC activation also potentiated the exocytosis stimulated by Ca^{2+} release from intracellular Ca^{2+} stores (*versus* Ca^{2+} influx through SOC). PDEC were treated with trypsin in the presence of both 500 nM BIS I to inhibit PKC and 10 μM La^{3+} to block SOC (Fig. 8*D*). In this setting BIS I treatment affected neither the $[Ca^{2+}]_i$ increase caused by Ca^{2+} mobilization (Fig. 8*D versus* Fig. 3*C*) nor exocytosis (3.4 ± 1.2, $n = 8$, with BIS I *versus* 2.7 ± 0.6 without BIS I in Fig. 5*C*, $p = 0.5$). Thus, the rapid $[Ca^{2+}]_i$ increase mediated by Ca^{2+} mobilization can evoke significant exocytosis by itself even without concomitant contribution from PKC.

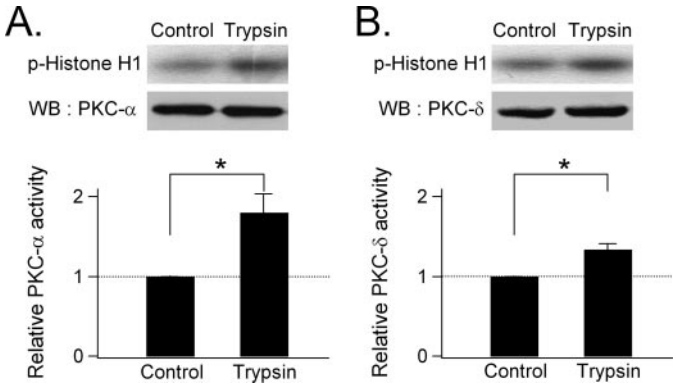

FIGURE 7. **Activation of PKC by trypsin.** A monolayer of PDEC was treated with 1 μM trypsin on both luminal and serosal sides for 2 min, and activities of the immunoprecipitated PKCα (*panel A*) and PKCδ (*panel B*) were determined by phosphorylation of histone H1. For each panel, the *upper rows* show phosphorylated (*P-*) histone, and the *lower rows* show the total amount of each kinase, as detected by Western blotting (*WB*). The relative PKC activity, normalized to the untreated control, is shown at the *bottom* of each *panel* ($n = 3$–4; *, $p < 0.05$).

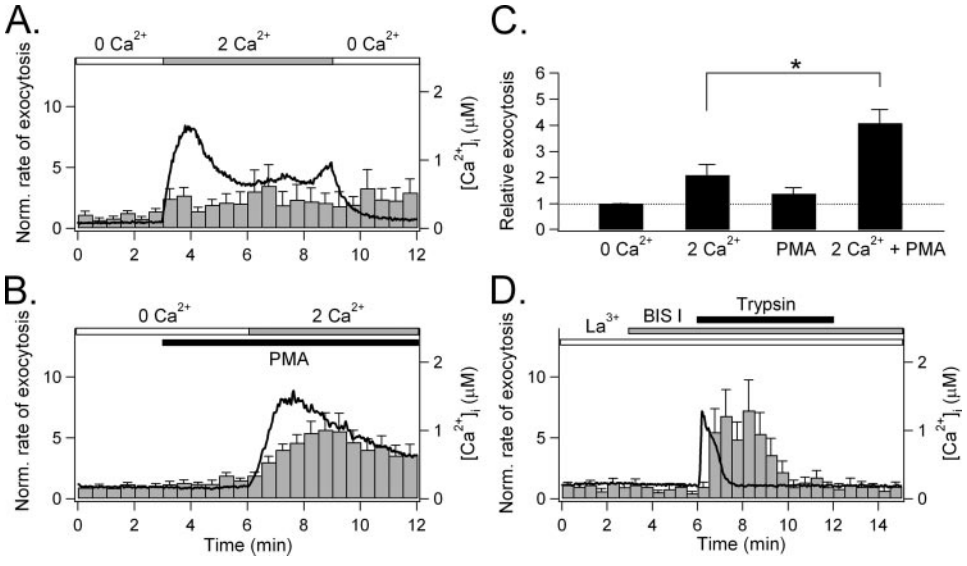

FIGURE 8. **Potentiation by PKC of exocytosis induced by Ca^{2+} influx.** *A*, stimulation of $[Ca^{2+}]_i$ increase and exocytosis by Ca^{2+} influx through SOC. PDEC were pretreated with 5 μM thapsigargin for 5 min to activate SOC before base line recording in Ca^{2+}-free Ringer's solution. Subsequent exposure to Ringer's solution containing 2 mM Ca^{2+} induced Ca^{2+} influx via the SOC (*solid line*, average of 5 experiments) and increased exocytosis (*histogram*, average of 12 experiments). *B*, stimulation of exocytosis by PKC. The experiment shown in *panel A* was repeated with an additional pretreatment with 10 nM PMA to activate PKC ($n = 3$). *C*, cross-talk between PKC activation and Ca^{2+} influx in stimulating exocytosis. Relative exocytosis during the first 3 min after stimulation in solutions containing 2 mM Ca^{2+}, PMA alone, and Ca^{2+} plus PMA are compared with that in a solution depleted of Ca^{2+} (0 Ca^{2+}); *, $p < 0.01$. *D*, exocytosis induced solely by Ca^{2+} mobilization from intracellular stores. PDEC were preincubated with 10 μM La^{3+} to block Ca^{2+} influx through SOC (*open bar*) and 500 nM BIS I to inhibit PKC (*gray bar*) before being treated with 1 μM trypsin (*solid bar*). The resulting effect of trypsin on $[Ca^{2+}]_i$ (*solid line*, $n = 3$) and exocytosis (histogram, $n = 8$) is shown.

Trypsin Mediates Exocytosis in PDEC via PAR-2—So far we have treated trypsin action as synonymous with PAR-2 activation. To demonstrate that direct PAR-2 activation gives the same responses, we used the AP for PAR-2 and, as control, a peptide with the reverse amino acid sequence (RP). AP stimulated increases in both $[Ca^{2+}]_i$ (Fig. 9*A*) and exocytosis (2.4 ± 0.7, $n = 13$, Fig. 9*D*), but RP did not stimulate an $[Ca^{2+}]_i$ increase (Fig. 9*A*). In separate experiments, 10 μM PAR-2 AP also increased the activity of PKCα (2.1 ± 0.4; $n = 3$; data not shown).

Trypsin is synthesized in pancreatic acinar cells and secreted into pancreatic ducts as inactive trypsinogen. Active trypsin is present in the pancreas only in mostly pathologic conditions where its concentration will be unpredictable. We, therefore, lowered the trypsin concentration from 1 μM to 100 and 10 nM to determine the active range. Even 10 nM trypsin reproducibly elicited

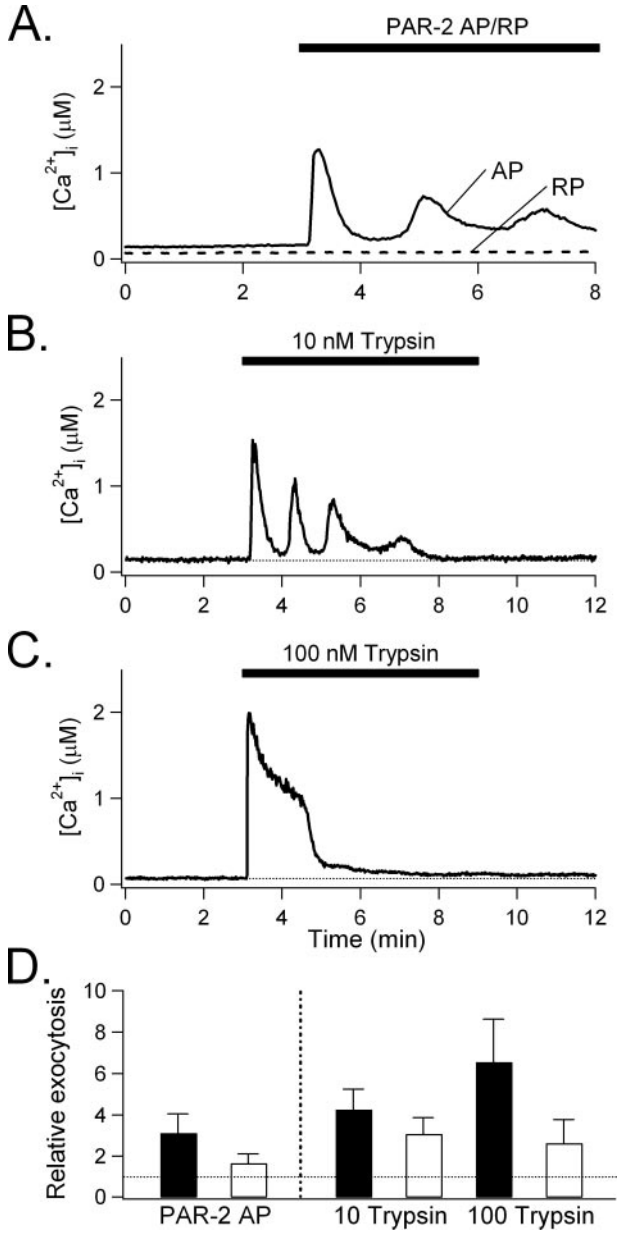

FIGURE 9. **PAR-2 expression and function on PDEC.** *A*, effects of PAR peptides on $[Ca^{2+}]_i$. PDEC were treated with 10 μM concentrations of either PAR-2 AP (*solid line*, a representative trace from four experiments) or PAR-2 RP (*dotted line*, a representative trace from six experiments). *B* and *C*, effect of low concentrations of trypsin on PDEC. $[Ca^{2+}]_i$ elevation in single PDEC induced by 10 nM (*B*, a representative trace from three experiments) or 100 nM trypsin (*C*, representative trace from four experiments). *D*, stimulation of exocytosis by 10 μM PAR2-AP or low concentrations of trypsin. The average relative exocytosis evoked by 10 nM ($n = 8$) or 100 nM ($n = 13$) trypsin is shown. Relative exocytosis was analyzed separately during the early (3–6 min, *filled bar*) and the late (6–9 min, *open bar*) phases to compare with those shown in Fig. 5*D*). The *broken line* indicates background exocytosis before trypsin treatment.

oscillating $[Ca^{2+}]_i$ increases (Fig. 9*B*) resembling the effect of 10 μM PAR-2 AP (Fig. 9*A*) and sufficient for inducing both an early and late increase in exocytosis (4.2 ± 1.0, $p = 0.01$, early phase; 3.1 ± 0.8, $p = 0.02$, late phase, $n = 8$, Fig. 9*D*). At a concentration of 100 nM, a sustained $[Ca^{2+}]_i$ increase was observed similar to the response evoked by 1 μM trypsin (Fig. 9*C*) and again sufficient for eliciting both early and late exocytosis (6.5 ± 2.1, early phase; 2.6 ± 1.1, late phase, $n = 13$, Fig. 9*D*).

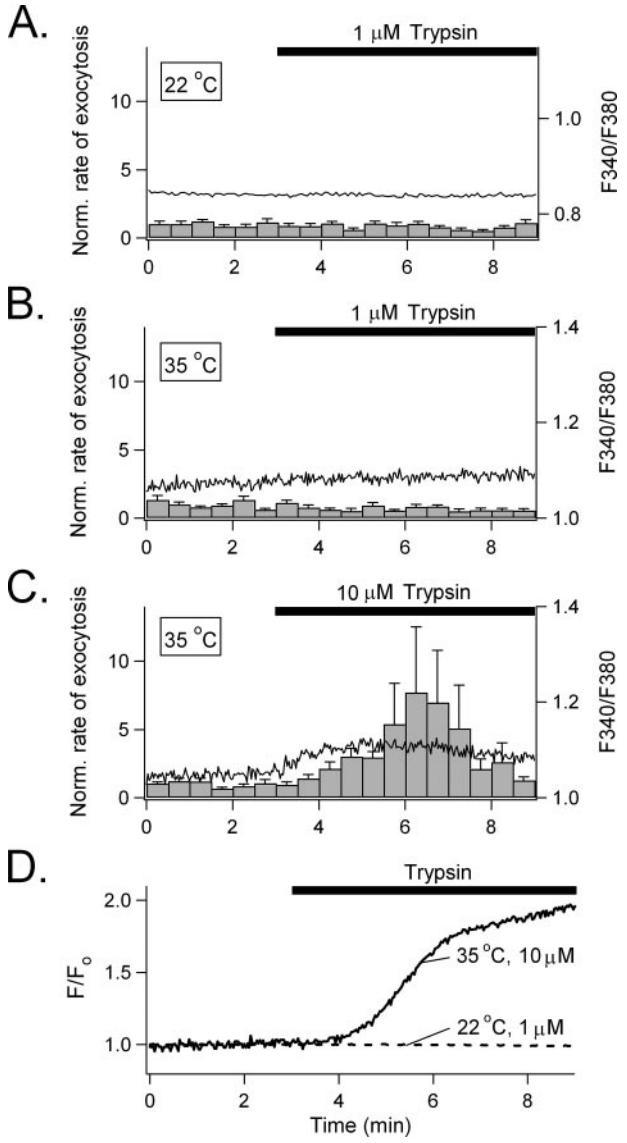

FIGURE 10. **Accessibility of serosal PAR-2 to very high luminal trypsin.** *A–C*, effect of luminal trypsin on luminal exocytosis from confluent PDEC monolayers. Luminal exocytosis, averaged from 4–8 experiments and determined by positioning a carbon fiber electrode on the apical membrane, is shown as *histograms* in *A–C*. *A*, 1 μM trypsin at 22 °C ($n = 8$). *B*, 1 μM trypsin at 35 °C ($n = 6$). *C*, 10 μM trypsin at 37 °C ($n = 4$). $[Ca^{2+}]_i$, averaged values are shown as a *solid tracing* in *panels A* ($n = 3$), *B* ($n = 4$), and *C* ($n = 4$). *D*, effect of luminal trypsin on paracellular permeability of macromolecules through confluent PDEC monolayers. Leak of dextran-fluorescein (5 μM, present in the luminal compartment) to the serosal compartment was monitored in the presence of luminal trypsin (either 10 μM at 35 °C or 1 μM at 22 °C) (see "Experimental Procedures"). The panel shows representative traces from 3–4 similar experiments.

Trypsin Acts Serosally through Basolateral PAR-2 in PDEC Monolayers—We previously demonstrated with immunofluorescence and electrophysiologic studies in Ussing chambers that PAR-2 is localized to the basolateral membrane of PDEC (7). Accordingly, 1 μM trypsin, applied to the luminal surface of confluent monolayers of polarized PDEC, failed to evoke exocytosis at both 22 and 35 °C (Fig. 10, *A* and *B*). A higher luminal concentration (10 μM) slowly increased exocytosis and $[Ca^{2+}]_i$ at 35 °C, probably because trypsin could break down the epithelial tight junctions, leak to the serosal compartment, and activate basolateral PAR-2 (Fig. 10*C*). Indeed, 10 μM trypsin at

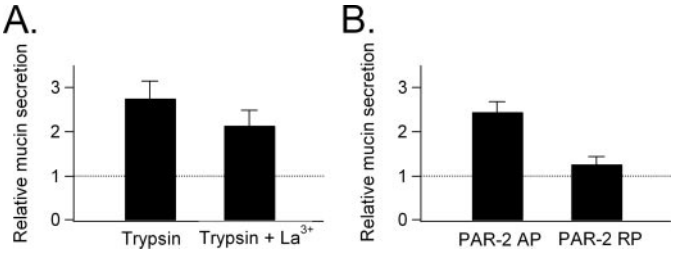

FIGURE 11. **Stimulation of mucin secretion by trypsin.** *A*, effect of trypsin on mucin secretion. Confluent PDEC were treated with 1 μM serosal trypsin for 1 h in Ringer's in the absence ($n = 10$) or presence of 10 μM La^{3+} ($n = 9$). The mucin released into the luminal medium was measured. The relative mucin secretion, normalized to untreated control and averaged, is shown. *B*, effect of PAR-2 AP and RP on mucin secretion. PDEC were treated with 1 μM concentrations of either serosal PAR-2 AP or serosal PAR-2 RP for 10 min, and the luminal mucin release was measured ($n = 3$).

35 °C induced a leak of fluorescein dextran (M_r 10,000, 5 μM) across the PDEC monolayers, whereas1 μM trypsin at 22 °C could not break the barrier (Fig. 10*D*). In addition, increased exocytosis paralleled increased fluorescein dextran permeability, with a delay of ~1 min after trypsin treatment.

PAR-2 Activation Induces Mucin Secretion—In PDEC, as in other epithelial cells, exocytosis may serve two general functions, delivery of membrane proteins to the plasma membrane (*e.g.* the vesicular H^+-ATPase) and secretion of products synthesized and stored within intracellular vesicles. Because PDEC contain mucin vesicles (10), we determined whether PAR-2 activation could induce mucin secretion. Trypsin (1 μM) was applied to the serosal side of PDEC monolayers for 1 h, and the [^{3}H]glucosamine-labeled mucin was released over the 1 h measured (Fig. 11*A*). Trypsin stimulated luminal mucin secretion by a factor of 2.7 ± 0.4 ($n = 10$) relative to base line. By comparison, mucin secretion evoked by trypsin in the presence of La^{3+} to block SOC was 2.1 ± 0.3 ($n = 9$, $p = 0.26$, Fig. 11*A*). Serosal PAR-2 AP (1 μM), but not RP, also stimulated luminal mucin secretion (2.4 ± 0.2-fold increase *versus* base line, $n = 3$, Fig. 11*B*), suggesting PAR-2 mediation of this effect of trypsin on mucin secretion.

DISCUSSION

In a previous report we established PAR-2 expression on the basolateral membrane of PDEC and its function in stimulating the Ca^{2+}-activated Cl^- and K^+ channels (7). In this report we define the different signaling pathways activated by PAR-2 and investigated how they interact to stimulate the complex function of exocytosis.

Trypsin-induced PAR-2 Signaling—In different tissues PAR-2 effects are typically mediated through PLC-mediated generation of IP_3 and DAG (3, 4); induction of a cAMP increase has also been suggested (16–18).

Using a sensitive fluorescence-based method, we failed to detect an increase of cAMP stimulated by trypsin and, thus, excluded a role for this pathway in the PAR-2 effect in dog PDEC. This finding is consistent with our previous observation that in these cells PAR-2 did not stimulate the cystic fibrosis transmembrane conductance regulator, a Cl^- channel typically activated through cAMP (7).

In contrast, using additional fluorescence markers to identify PIP_2/IP_3 and DAG, we demonstrated that PLC hydrolyzes PIP_2 on the plasma membrane to generate cytoplasmic IP_3 and plasma membrane-bound DAG. The expected effects of IP_3 on increased $[Ca^{2+}]_i$ and of DAG on PKC activation were also demonstrated. Thus, PAR-2 activation by trypsin caused a biphasic increase in $[Ca^{2+}]_i$ measured in real-time with Indo-1. The first phase, which peaks rapidly and decays in about 2 min, is independent of extracellular Ca^{2+}; it likely results from Ca^{2+} mobilization from intracellular stores triggered by IP_3. This phase is followed by a sustained, but smaller $[Ca^{2+}]_i$ increase. This second phase is abolished by extracellular Ca^{2+} removal and is blocked by La^{3+}. It must result from Ca^{2+} influx through SOC activated after Ca^{2+} mobilization depletes intracellular Ca^{2+} stores. In addition, immunoprecipitation and a functional assay using histone phosphorylation demonstrated activation of both PKCα and PKCδ as the downstream mediators of DAG generated by PAR-2 activation.

Effects of Trypsin and PAR-2 Activation on Exocytosis—In previous studies $[Ca^{2+}]_i$ increase by PAR-2 activation stimulated Ca^{2+}-activated ion channels in PDEC (7), whereas PKC activated by PAR-2 modulated the expression and function of TRPV1 in neurons (16). With the dog PDEC used in this report, we have also demonstrated regulated exocytosis by both Ca^{2+} and PKC signals (8). To integrate these findings, we have examined in this report how the different signaling pathways activated by PAR-2 interact to induce exocytosis, an important and complex function in PDEC.

Trypsin stimulated a biphasic increase in the rate of exocytosis, mirroring the biphasic $[Ca^{2+}]_i$ increase; that is, a fast peaked increase followed by a more modest but sustained increase. The late sustained increase is due to the $[Ca^{2+}]_i$ increase resulting from SOC-mediated Ca^{2+} influx, and it was abolished by depletion of extracellular Ca^{2+} and by La^{3+}. The early peak exocytosis increase is partially dependent on Ca^{2+} mobilization from intracellular stores, as it was partly inhibited by BAPTA-AM, which chelates intracellular Ca^{2+}, or by thapsigargin, which depletes intracellular Ca^{2+} stores.

The residual Ca^{2+}-independent increase in exocytosis that persisted after BAPTA treatment was not fully unexpected since we previously established in PDEC that activated protein kinases could stimulate exocytosis (8). This Ca^{2+}-independent exocytosis was likely mediated by PKC-dependent phosphorylation. It was blocked by PKC inhibition and accompanied by activation of PKCα and PKCδ.

When SOC was activated by depletion of intracellular Ca^{2+} stores and Ca^{2+} influx occurred (2 mM extracellular Ca^{2+}), the resulting small increase in $[Ca^{2+}]_i$ was sufficient to stimulate exocytosis modestly. Activation of PKC with 10 nM PMA alone caused a minor increase in exocytosis; Ca^{2+} influx boosted its effect on exocytosis. This effect is also consistent with the stronger stimulation of exocytosis observed when SOC and PKC was simultaneously activated by trypsin (Fig. 5*A* *versus* 8, *A* and *B*). The mechanisms underlying this cross-talk are beyond the scope of this report but constitute an important area for future investigation. Amadesi *et al.* (16) recently observed that PAR-2 can activate PKCϵ to sensitize TRPV1 in cultured dorsal root ganglia neurons and HEK 293 cells, suggesting a possible activation of multiple PKC subtypes by PAR-2.

Significance of the PAR-2 Effect on Exocytosis in PDEC—PAR-2 is widely expressed in the cardiovascular, immune, nervous, respiratory, and gastrointestinal systems, where it achieves diverse physiological and pathological functions (2, 5, 24). Studies of PAR-2 function have mainly concentrated on ion transport, muscle contractility, and neurotransmission. This report adds vesicular exocytosis to this repertoire of functions. In PDEC, exocytosis serves two general functions, the delivery and integration of membrane proteins into the plasma membrane and the extracellular discharge and secretion of molecules contained in these vesicles. In pig PDEC, vesicular fusion stimulated by cAMP inserts vacuolar H^+-ATPases in the basolateral membrane, allowing serosal H^+ secretion; this function compensates for luminal HCO_3^- secretion when these cells are stimulated with secretin (25). This exocytotic function was not studied further here because PAR-2 activation did not seem to increase cAMP. On the other hand, the dog PDEC studied in this report contain large mucin granules and have been shown to secrete mucin (10). By monitoring the release of [^{3}H]glucosamine-labeled glycoproteins, we demonstrated that trypsin also activates PAR-2 to stimulate mucin secretion. Variability of mucin release from different monolayers precluded the accurate detection of small inhibitory effects by blockers; however, the overall parallel stimulation of exocytosis and mucin secretion mediated by PAR-2 (Fig. 11) suggests that the exocytosis investigated in this report has a role in mucin secretion.

Studies using biliary and cerulein induced pancreatitis have suggested that PAR-2 activation may serve a protective role in diminishing the severity of pancreatic parenchymal injury (26, 27). This protective effect is partially related to the ability of PAR-2 to stimulate the secretion of trypsin by acinar cells (28). We previously postulated that the PAR-2-mediated stimulation of fluid and electrolyte secretion by PDEC could be an additional mechanism for the pancreas to dilute and wash out noxious agents. It is possible that the promotion of exocytosis and mucin secretion may be an additional cellular protective mechanism (29).

Acknowledgments—We thank N. W. Bunnett for helpful discussions, C. E. Savard for the design of mucin assay, and T. Wong for cell culture.

REFERENCES

1. Nystedt, S., Emilsson, K., Wahlestedt, C., and Sundelin, J. (1994) *Proc. Natl. Acad. Sci. U. S. A.* **91,** 9208–9212
2. Ossovskaya, V. S., and Bunnett, N. W. (2004) *Physiol. Rev.* **84,** 579–621
3. Böhm, S. K., Kong, W., Brömme, D., Smeekens, S. P., Anderson, D. C., Connolly, A., Kahn, M., Nelken, N. A., Coughlin, S. R., Payan, D. G., and Bunnett, N. W. (1996) *Biochem. J.* **314,** 1009–1016
4. Böhm, S. K., Khitin, L. M., Grady, E. F., Aponte, G., Payan, D. G., and Bunnett, N. W. (1996) *J. Biol. Chem.* **271,** 22003–22016
5. Nguyen, T. D. (2004) *Gastroenterology* **126,** 1907–1909
6. Vergnolle, N. (2000) *Aliment. Pharmacol. Ther.* **14,** 257–266
7. Nguyen, T. D., Moody, M. W., Steinhoff, M., Okolo, C., Koh, D.-S., and Bunnet, N. W. (1999) *J. Clin. Investig.* **103,** 261–269
8. Koh, D.-S., Moody, M. W., Nguyen, T. D., and Hille, B. (2000) *J. Gen. Physiol.* **116,** 507–519
9. Jung, S.-R., Kim, M.-H., Hille, B., Nguyen, T. D., and Koh, D.-S. (2004) *Am. J. Physiol. Cell Physiol.* **286,** 573–579
10. Oda, D., Savard, C. E., Nguyen, T. D., Eng, L., Swenson, E. R., and Lee, S. P. (1996) *Am. J. Pathol.* **148,** 977–985
11. Koh, D.-S., and Hille, B. (1997) *Proc. Natl. Acad. Sci. U. S. A.* **94,** 1506–1511
12. Nikolaev, V. O., Bünemann, M., Hein, L., Hannawacker, A., and Lohse, M. J. (2004) *J. Biol. Chem.* **279,** 37215–37218
13. Grynkiewicz, G., Peonie, M., and Tsien, R. Y. (1985) *J. Biol. Chem.* **260,** 3440–3450
14. Kim, K.-T., Koh, D.-S., and Hille, B. (2000) *J. Neurosci.* **20,** RC101, 1–5
15. Koh, D.-S., and Hille, B. (1999) *J. Neurosci. Methods* **88,** 83–91
16. Amadesi, S., Cottrell, G. S., Divino, L., Chapman, K., Grady, E. F., Bautista, F., Karanjia, R., Barajas-Lopez, C., Vanner, S., Vergnolle, N., and Bunnett, N. W. (2006) *J. Physiol.* (*Lond.*) **575,** 555–571
17. Scott, G., Leopardi, S., Parker, L., Babiarz, L., Seiberg, M., and Han, R. (2003) *J. Investig. Dermatol.* **121,** 529–541
18. Gatti, R., Andre, E., Amadesi, S., Dinh, T. Q., Fischer, A., Bunnett, N. W., Harrison, S., Geppetti, P., and Trevisani, M. (2006) *J. Appl. Physiol.* **101,** 506–511
19. Nguyen, T. D., Meichle, S., Kim, U. S., Wong, T., and Moody, M. W. (2001) *Am. J. Physiol. Gastrointest. Liver Physiol.* **280,** 795–804
20. Horowitz, L. F., Hirdes, W., Suh, B.-C., Hilgemann, D. W., Mackie, K., and Hille, B. (2005) *J. Gen. Physiol.* **126,** 243–262
21. Rychkov, G. Y., Litjens, T., Roberts, M. L., and Barritt, G. J. (2005) *Cell Calcium* **37,** 183–191
22. Nguyen, T. D., Moody, M. W., Savard, C. E., and Lee, S. P. (1998) *Am. J. Physiol. Gastrointest. Liver Physiol. 2* **75,** 104–113
23. Gschwendt, M., Müller, H. J., Kielbassa, K., Zang, R., Kittstein, W., Rincke, G., and Marks, F. (1994) *Biochem. Biophys. Res. Commun.* **199,** 93–98
24. Kawabata, A., Kuroda, R., Nishida, M., Nagata, N., Sakaguchi, Y., Kawao, N., Nishikawa, H., Arizono, N., and Kawai, K. (2002) *Life Sci.* **71,** 2435–2446
25. Villanger, O., Veel, T., and Raeder, M. G. (1995) *Gastroenterology* **108,** 850–859
26. Namkung, W., Han, W., Luo, X., Muallem, S., Cho, K., Kim, K., and Lee, M. (2004) *Gastroenterology* **126,** 1844–1859
27. Sharma, A., Tao, X., Gopal, A., Ligon, B., Andrade-Gordon, P., Steer, M. L., and Perides, G. (2005) *Am. J. Physiol. Gastrointest. Liver Physiol.* **288,** 388–395
28. Singh, V. P., Bhagat, L., Navina, S., Sharif, R., Dawra, R. K., and Saluja, A. K. (2007) *Gut* **56,** 958–964
29. Allen, A., Flemström, G., Garner, A., and Kivilaakso, E. (1993) *Physiol. Rev.* **73,** 823–857